

Nanosphere Lithography: Self-Assembled Photonic and Magnetic Materials

Amanda J. Haes, Christy L. Haynes, Richard P. Van Duyne

Department of Chemistry, Northwestern University
Evanston, IL 60208-3113, U.S.A.

ABSTRACT

Early work with size-tunable periodic particle arrays (PPAs) fabricated by nanosphere lithography (NSL) demonstrated that the localized surface plasmon resonance (LSPR) could be tuned throughout the visible region of the spectrum. Further developments of the NSL technique have produced a myriad of nanoparticle configurations. Presented in this paper are several array types and examples of their utility in current applications. Both the sensitivity and tunability of the LSPR have been firmly established using single layer PPAs. Magnetic force microscopy (MFM) has been used to show that double layer PPAs act as single domain magnets and give strong MFM contrast. Angle-resolved NSL has produced nanogap and nano-overlap structures with manipulation resolution of one nanometer. Nanowell structures extend the original two-dimensional structure into the third dimension. Exploitation of this flexible, materials-general NSL technique allows for investigation of the catalytic, electrochemical, magnetic, optical and thermodynamic properties of nanoparticles.

INTRODUCTION

Nanoparticles composed of metals and semiconductors exhibit distinct size-dependent chemical and physical properties that differ from their bulk material counterparts. Understanding these properties and developing low cost, high-efficiency production methods are motivating factors in this line of research.

Several standard lithographic methods are routinely used to create nanostructures with controlled size, shape, and spacing. UV photolithography [1,2] is a widely used method; however, its feature sizes are limited by its diffraction-limit of $\lambda/2$. Electron beam lithography [2] is characterized by low sample output, high sample cost, modest feature shape control, and excellent feature size control. X-ray lithography [3] is characterized by initially high capital costs but high sample throughput. Additional lithographic techniques are in development. Among these methods are scanning tunneling microscopy [4] and atomic force microscopy [5] lithographic techniques. As a consequence of the aforementioned limitations, alternative, parallel nanolithographic techniques are being explored including (1) diffusion-controlled aggregation at surfaces [6]; (2) laser focused atom deposition [7]; (3) chemical synthesis of metal-cluster compounds and semiconductor nanocrystals [8]; and (4) "natural lithography" [9,10].

The work presented here is an extension of Deckman's "natural lithography," hereafter renamed nanosphere lithography (NSL) [11]. NSL is inexpensive (less than \$1 per sample), inherently parallel, high-throughput, and materials general technique. Consequently, NSL is capable of producing well-ordered, 2D periodic arrays of nanoparticles from a wide variety of materials on many substrates.

In this paper, demonstrations of multiple NSL structures will be presented. The size-tunable optical properties of single layer periodic particle arrays (PPAs) [12] and the magnetic properties

of double layer PPAs will be exploited [13]. Additionally, by angle-resolving the nanosphere mask, nanogap, nano-overlap, and nanochain structures can be fabricated [13]. Finally, by combining reactive ion etching (RIE) with NSL, nanowell structures can be fabricated.

EXPERIMENTAL

Materials. Ag wire (99.99%), 0.50 mm diameter was purchased from D.F. Goldsmith (Evanston, IL). Ni foil (99.994%) was purchased from Alfa AESAR (Ward Hill, MA) and Co foil (99.95%) was purchased from Aldrich Chemical Company (Milwaukee, WI). Ruby red muscovite mica was purchased from Asheville-Schoonmaker (Newport News, VA) in the form of 50 μm thick sheets. Borosilicate glass substrates were Fisherbrand No. 2 cover slips from Fisher Scientific. Tungsten vapor deposition boats were acquired from R. D. Mathis (Long Beach, CA). Polystyrene nanospheres of various diameters were purchased from Interfacial Dynamics Corporation (Portland, OR). Triton X-100 was obtained from Aldrich (Milwaukee, WI). For all steps of substrate preparation, water purified with cartridges from Millipore (Marlborough, MA) to a resistivity of 18 $\text{M}\Omega$ was used.

Substrate preparation. Mica substrates of approximately 1 cm^2 in area and 50 μm thickness were either used as received or freshly cleaved immediately before nanosphere mask formation. Glass substrates were cleaned by immersion in piranha solution (3:1 concentrated H_2SO_4 :30% H_2O_2) at 80 $^\circ\text{C}$ for 1 hour. After cooling, the substrates were rinsed repeatedly with millipure water and then sonicated for 60 minutes in 5:1:1 H_2O : NH_4OH :30% H_2O_2 solution. Following sonication, the substrates were again rinsed repeatedly with water and then used immediately or stored in water for no longer than one week.

Periodic particle array preparation. Simply, a suspension of nanospheres was dropcoated onto the substrate where they self-assembled into a hexagonally close-packed 2D colloidal crystal that served as a deposition mask. For nanoparticle arrays fabricated on mica substrates, the nanospheres were received as a suspension in water and were then further diluted in a 1:1 ratio with a solution of the surfactant Triton X-100 and methanol (1:400 by volume). Addition of the surfactant solution allowed for better packing over large areas of the mica substrate. Nanospheres used to form deposition masks on glass substrates were used as received without any further dilution with a surfactant solution. Once the 2D colloidal crystal deposition mask was formed, the substrates were mounted into the chamber of a consolidated Vacuum Corporation vapor deposition system. The angle-resolved deposition was accomplished by mounting the sample on machined Al blocks. Ag films of various thicknesses were then deposited over the nanosphere mask. The mass thickness, d_m , for each film was measured using a Leybold Inficon XTM/2 deposition monitor quartz crystal microbalance (East Syracuse, NY). After the Ag deposition, the nanosphere mask was removed by sonicating the entire substrate in either CH_2Cl_2 or absolute ethanol for 2 minutes.

Atomic force microscopy (AFM) measurements. AFM images were collected under ambient conditions using a Digital Instruments Nanoscope III microscope operating in either contact mode or tapping mode. Etched Si nanoprobe tips (Digital Instruments, Santa Barbara, CA) with spring constants of approximately 0.15 N M^{-1} were used. These conical shaped tips had a cone angle of 20 $^\circ$ and an effective radius of curvature of 10 nm. The resonance frequency of the tapping mode cantilevers was measured to be between 280 and 330 kHz. The AFM images presented here represent raw, unfiltered data.

Ultraviolet-visible extinction spectroscopy. Extinction spectra were recorded in standard transmission geometry using either a Beckman DU-7, Ocean Optics SD2000, or an OLIS modified Cary 14 spectrophotometer. Regardless of the instrument used, all macroextinction measurements were recorded using unpolarized light with a probe beam size of approximately 2-4 mm².

Magnetic force microscopy (MFM) measurements. MFM images were collected under ambient conditions using a Digital Instruments Multimode Nanoscope IIIa microscope. MESP MFM tips (Digital Instruments, Santa Barbara, CA) were vertically magnetized using the device provided by Digital Instruments. The samples were magnetized by placing them between two 3/4 inch disk magnets. The magnetic field between these two magnets is approximately 4000 Oe.

Pulsed laser deposition of Ni and Co. The 532 nm or 1064 nm output of a Quanta-Ray DCR-1 Nd:YAG laser was used to perform the deposition. The turbo pumped vacuum chamber had a base pressure of 1×10^{-6} torr. The laser pulses were 10 ns in duration at a rate of 10 Hz with an energy of 7.5 to 10 mJ/pulse. The film thickness was continuously monitored using a quartz crystal microbalance, and the deposition rate was typically 0.1 nm/minute. Once the desired deposition mass thickness, d_m , was achieved, the samples were removed from the vacuum chamber, and the nanospheres were removed by dissolution in CH₂Cl₂ with the aid of sonication.

Reactive Ion Etching. The 2D colloidal crystal deposition masks were mounted into the chamber of a home-built RIE chamber. The substrate was then etched with 20 mTorr CF₄ at 2.2 W/cm² for varied lengths of time.

DISCUSSION

Single layer periodic particle arrays. In the simplest case of NSL, a single monolayer of hexagonally close-packed nanospheres is deposited onto the substrate. Following material deposition through the sphere mask and sphere removal, an array of triangular particles is created. This nanoparticle pattern, which covers 7.2% of the substrate area, is referred to as a single layer periodic particle array (SL PPA).

The signature optical property of noble metal nanoparticles is the localized surface plasmon

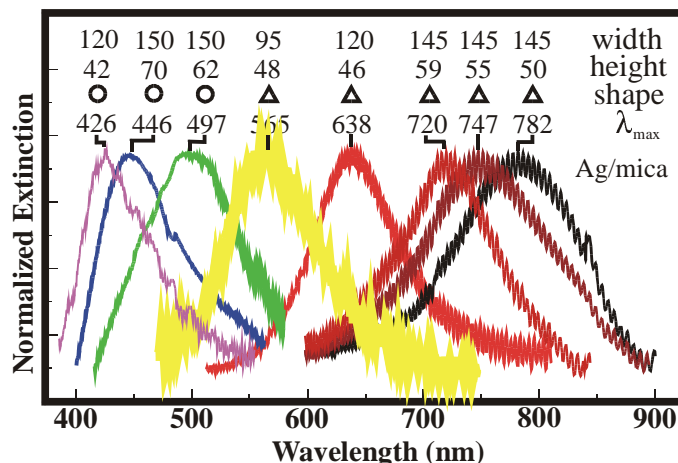


Figure 1. UV-vis extinction spectra of Ag nanoparticle arrays on mica substrates.

resonance, hereafter, LSPR. The primary consequences of the LSPR excitation are (1) selective photon absorption and scattering and (2) electromagnetic field enhancement. The LSPR of SL PPAs, as monitored by extinction spectroscopy, has been shown to be tunable from ~400 nm to 6000 nm [12]. Figure 1 depicts this tunability throughout the visible range. This was accomplished by varying the size and shape of the nanoparticles.

Double layer periodic particle arrays. By increasing the concentration of nanospheres deposited onto the substrate, two layers of hexagonally close-packed nanospheres form a

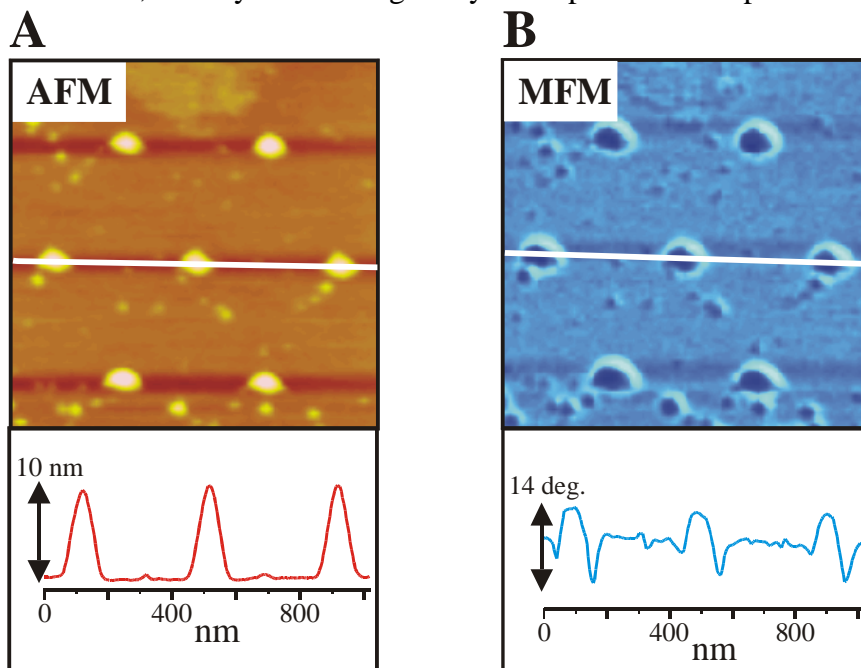


Figure 2. Topographic and magnetic force image of a double layer Ni nanoparticle array $D = 401$ nm, $d_m = 10$ nm. A) $1 \times 1 \mu\text{m}$ topographic image of a double layer array and corresponding linescan, B) $1 \times 1 \mu\text{m}$ magnetic force image of the array and corresponding linescan.

colloidal crystal. Following metal deposition through the sphere mask and subsequent sphere removal, an array of hexagonal particles is created. This nanoparticle pattern, which covers 2.2% of the substrate, is referred to as a double layer periodic particle array (DL PPA).

As magnetic materials reach the size regime of 100-500 nm, the physical size of the magnet dictates that the lowest energy structure is one in which all magnetic moments point in the same direction, creating a single domain magnet. Magnetic force microscopy (MFM) investigations of DL PPAs (particles with and approximate diameter of 20 nm) have demonstrated that these particles are single domain in nature (Figure 2) [13]. The most promising application of this architecture is their possible use for data storage.

Angle-resolved periodic particle arrays. In the aforementioned nanostructures, all materials were deposited from a source perpendicular to the nanosphere mask. By varying the angle between the nanosphere mask and the beam of deposition material, Θ_{dep} , a new class of NSL structures has been fabricated. This technique is referred to as angle-resolved NSL (AR NSL).

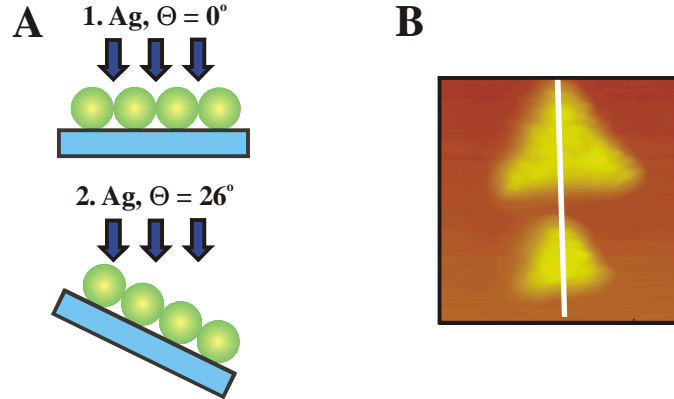


Figure 3. Angle-resolved nanosphere lithography. A) Depiction of angle-tuned masks, B) AFM image of a 25 nm nanogap between two Ag nanoparticles.

Nanogap architectures are fabricated by depositing metal through a nanosphere mask mounted at $\Theta_{\text{dep}} = 0^\circ$ and then depositing a second material (of the same or different composition) at or above a nanogap threshold value of Θ_{dep} . Figure 3 depicts a nanogap example in which Ag was deposited at $\Theta_{\text{dep}} = 0^\circ$ and 26° . The gap between these particles is approximately 25 nm. By varying the second Θ_{dep} in 0.1° increments, the gap's spacing can be controlled with 0.75 nm resolution [13]. The gap between these particles can be varied so they are in contact or overlapping [13]. The possibility of performing more than two depositions using AR NSL also exists. By performing three depositions at different Θ_{dep} , nanochain structures can be made [13].

Nanowell structures. In a slightly different approach, a single monolayer of hexagonally close-packed nanospheres is deposited onto the substrate. Next, the samples were placed in a reactive ion etching (RIE) chamber and exposed to CF_4 plasma. When CF_4 plasma strikes the polystyrene nanospheres, the hydrocarbons are fluorinated. This non-volatile product is not

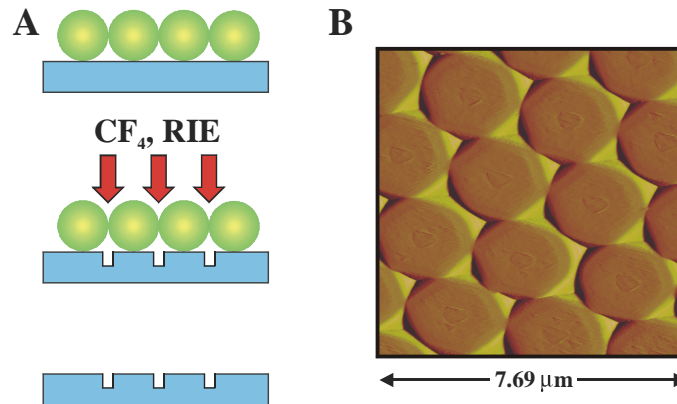


Figure 4. Nanowells by nanosphere lithography and reactive ion etching (RIE). A) RIE scheme, B) AFM image of nanowells.

etched away, so the spheres act as an etch stop. Meanwhile, as the CF₄ plasma penetrates the holes in the sphere mask, volatile SiF₂ radicals and SiF_x products are etched away [14]. After removing the sphere mask, AFM revealed triangular holes (nanowells) in the substrate (Figure 4). By depositing metal into the wells before nanosphere removal, homogeneous nanorods embedded in a substrate can be made and studied.

CONCLUSIONS

Nanosphere lithography (NSL) has been used to fabricate a variety of nanoparticle structures. The localized surface plasmon resonance of single layer periodic particle arrays have been shown to be tunable throughout ~ 400 nm - 6000 nm. Double layer periodic particle arrays exhibit single domain magnet properties. Nanogap, nano-overlap, and nanochain structures can be made using angle-resolved techniques. By combing NSL with reactive ion etching, nanowell structures can be fabricated.

NSL is a powerful fabrication technique that produces arrays of nanoparticles with controlled shape, size, and interparticle spacing. The development of NSL is driven by the need to produce a homogenous, materials-general nanoparticle synthetic technique. We anticipate that the inexpensive and flexible nature of this technique will be a powerful tool in the advancement of nanoparticle understanding.

ACKNOWLEDGEMENTS

The authors would like to acknowledge Michelle Malinsky, Traci Jensen, and Matt Smith for their work, John Ketterson for the use of the RIE chamber, and Joseph Hupp for providing access to the Cary 14 spectrophotometer. This research was supported by the MURI ARO (Grant DAAG55-97-1-0133), NSF (Grant CHE-940078), and MRSEC program of the NSF (Grant DMR-9632472 and DMR-0076097).

REFERENCES

1. G. M. Wallraff, W. D. Hinsberg, *Chem. Rev.*, **99**, 1801-1821 (1999).
2. T. Ito, S. Okazaki, *Nature*, **406**, 1027-1031 (2000).
3. H. I. Smith, M. L. Schattenburg, *IBM J. Res. Develop.*, **37**, 319-329 (1993).
4. J. A. Stroschio, D. M. Eigler, *Science*, **254**, 1319-1326 (1991).
5. G. Y. Liu, S. Xu, Y. Qian, *Acc. Chem. Res.*, **33**, 457-466 (2000).
6. H. Roder, E. Hahn, H. Brune, J. P. Bucher, K. Kern, *Nature*, **366**, 141-143 (1993).
7. J. J. McClelland, R. E. Scholten, E. C. Palm, R. J. Celotta, *Nature*, **262**, 877-880 (1993).
8. F. Mulder, T. Stegink, L. de Jongh, G. Schmid, *Nature*, **367**, 716-718 (1994).
9. H. Fang, R. Zeller, P. J. Stiles, *Appl. Phys. Lett.*, **55**, 1433-1435 (1989).
10. H. W. Deckman, J. H. Dunsmuir, *Appl. Phys. Lett.*, **41**, 377-379 (1982).
11. J. C. Hulteen, R. P. Van Duyne, *J. Vac. Sci. Technol. A*, **13**, 1553-1558 (1995).
12. T. R. Jensen, M. D. Malinsky, C. L. Haynes, R. P. Van Duyne, *J. Phys. Chem. B*, **104**, 10549-10556 (2000).
13. M. T. Smith, Northwestern University Ph.D. Thesis (1999).
14. G. Cunge, P. Chabert, J. Booth, *Plasma Sources Science and Technology*, **6**, 349-360 (1997).